DOE/ET-53088-159 IFSR #159

ROLE OF MULTIPLE HELICITY NONLINEAR INTERACTION OF TEARING MODES IN DYNAMO AND ANOMALOUS THERMAL TRANSPORT IN THE REVERSED FIELD PINCH

Z.G. An, P.H. Diamond, R.D. Hazeltine, J.N. Leboeuf, M.N. Rosenbluth, R.D. Sydora, T. Tajima, B.A. Carreras, L. Garcia, T.C. Hender, H.R. Hicks, J.A. Holmes V.E. Lynch, and H.R. Strauss

Institute for Fusion Studies
The University of Texas
Austin, Texas 78712

October 1984

*Revised version of paper presented at IAEA Conference, London, 1984

ROLE OF MULTIPLE HELICITY NONLINEAR INTERACTION OF TEARING MODES IN DYNAMO AND ANOMALOUS THERMAL TRANSPORT IN THE REVERSED FIELD PINCH

Z.G. An*, P.H. Diamond, R.D. Hazeltine, J.N. Leboeuf, M.N. Rosenbluth,
R.D. Sydora, T. Tajima
Institute for Fusion Studies
University of Texas
Austin, Texas 78712

B.A. Carreras, L. Garcia, T.C. Hender, H.R. Hicks,
J.A. Holmes, V.E. Lynch,
Oak Ridge National Laboratory
Oak Ridge, Tennessee 37831

H.R. Strauss
Courant Institute of Mathematical Sciences
New York University
New York, New York 10012

Abstract

A theory of magnetic fluctuation dynamics, the dynamo mechanism, and anomalous thermal transport in the Reversed Field Pinch is presented. Nonlinear generation of and coupling to $m \geqslant 2$ modes is advanced as an $m=1$ tearing modes sustain the magnetic configuration and stabilize themselves by lowering the safety factor on axis $(q(0))$ are elucidated. The nonlinear dynamics of resistive interchange modes is discussed. Stochastic magnetic field transport arguments are used to estimate anomalous thermal conductivity and confinement scalings.

*Permanent Address: The Southwestern Institute of Physics, Leshan, Sichuan, People's Republic of China.

1. INTRODUCTION

Recently, results from several Reversed Field Pinch (RFP) experiments have shed light on the structure of the observed magnetic fluctuations[1,2,3], their role in dynamo activity[4], and, in at least one case[1], their relation to anomalous thermal transport. It is widely believed that resistive tearing and interchange instabilities drive the magnetic fluctuations. Thus, a theory of the nonlinear evolution of interacting tearing modes is required for an understanding of RFP operation. In this paper, the results of several theoretical and computational investigations of the multiple helicity nonlinear interaction of tearing and resistive interchange modes are summarized. The implications of these results for models of dynamo activity and anomalous thermal transport are discussed.

This paper is divided into five sections. Section 2 contains a presentation of the plasma model. The dynamics of m=1 tearing modes is discussed in Section 3. In Section 3.1, the theory of multiple helicity nonlinear tearing mode interaction is presented. In Section 3.2, the magnetic field profile modification induced by m=1 tearing modes is addressed. Mechanisms for dynamo activity (α-effect) and quasilinear saturation are described. Section 4 contains a discussion of the nonlinear evolution of resistive interchange modes. In Section 5, the implications of the results of Section 3 and 4 for anomalous thermal transport are discussed.

2. PLASMA MODEL - REDUCED MHD FOR RFP

The parameters of current RFP discharges indicate that resistive MHD is an adequate plasma model. Recently, a new set of reduced resistive MHD equations for RFP plasmas has been derived.[5] These equations,

$$\frac{\partial\psi}{\partial t} = \underline{B} \cdot \underline{\nabla}\, \varphi + \eta C \tag{1}$$

$$\frac{D}{Dt}\, \underline{\nabla} \cdot \frac{\rho}{B^2}\, \underline{\nabla}\varphi = \underline{B} \cdot \underline{\nabla}(C - \langle\underline{J}\rangle \cdot \langle\underline{B}\rangle / \langle\underline{B}\rangle^2) \tag{2}$$

$$(\nabla_\vartheta^2 + \nabla_z^2)\chi = \langle\underline{B}\rangle \cdot \underline{\nabla}(\partial\psi/\partial r) \tag{3}$$

for the fluid stream function φ, the parallel vector potential component ψ, and χ, determined from the condition of radial force balance, describe the basic dynamics of RFP plasmas. Here $C = (1/\langle\underline{B}\rangle^2)\underline{\nabla} \cdot (\langle\underline{B}\rangle^2 \underline{\nabla}\psi - \langle\underline{B}\rangle\langle\underline{B}\rangle \cdot \nabla\psi - \langle\underline{B}\rangle \cdot \underline{\nabla}\chi\underline{\nabla}r)$ is the perturbed parallel current (J), $\langle\underline{B}\rangle$ and $\underline{B}$ are the average and total magnetic field, ρ is the density and η is the resistivity. Throughout this paper, times and lengths are normalized to τ_A and a, respectively, so that $S^{-1} = \tau_A/\tau_R$, where $\tau_A^{-1} = |\langle\underline{B}\rangle|/(4\pi\rho)^{1/2}a$ and $\tau_R^{-1} = \eta/a^2$. A cylindrical model with coordinates r, ϑ, z is used, and all fluctuations are expanded in toroidal (n) and poloidal (m) harmonics, so that $\underline{k} \cdot \langle\underline{B}\rangle = k_\parallel = (\langle B_\vartheta\rangle/r)(m - nq(r)) \cong -(\langle B_\vartheta\rangle/r)(nq'x)$. Computational solutions of these equations manifest the basic properties of RFP dynamics.

3. DYNAMICS OF M=1 TEARING MODES

3.1 Theory of Multiple Helicity Nonlinear Interaction

In the RFP, where the safety factor $q(r)$ decreases monotonically in radius, a spectrum of $m=1$ tearing modes, with $10<n<20$ and resonant surfaces within the reversal surface (see Figure 1a), is destabilized by resistive diffusion of the magnetic configuration[6] away from a Taylor state[7], thus resulting in the formation of magnetic islands. Due to the proximity of neighboring rational surfaces, where $q(r_1)=1/n$ and $q(r_2)=1/n+1$, respectively, the islands overlap for fluctuation levels of $(\delta B_r/B_o)\cong\varepsilon/n^2rq'\sim\varepsilon^2$, where $\varepsilon=a/R$. For $\varepsilon\sim1/4$, island overlap occurs at fluctuation levels less than that which are observed.[1] Indeed, for $S\leqslant10^5$, neighboring magnetic islands overlap while the tearing modes are still in the linear growth phase. Thus, strong nonlinear mode interaction, which generates turbulence and magnetic field line stochasticity, occurs throughout the RFP core.

As a consequence of the nonlinear interaction of the islands formed at r_1 and r_2, an $m=2$, $n'=2n+1$ current sheet and island are resonantly driven (see Figure 1b). The $m=2$, $n'=2n+1$ mode is linearly stable ($\Delta'_{m=2}<0$) and is further stabilized by flattening of the equilibrium current gradient by (global) $m=1$ modes. Thus, the driven (stable) $m=2$ modes nonlinearly absorb energy from the primary $m=1$ modes, which saturate when the rate of coupling of energy to $m=2$ balances the rate of equilibrium magnetic energy release by $m=1$'s.

This progressive current filamentation process (cascade) continues with the generation of $m \geq 3$, and eventually terminates when the driving energy (tapped through m=1 modes) is resistively dissipated at small scales and depleted by quasilinear profile modification.

The natural methods for theoretical analysis of these phenomena are those of renormalized turbulence theory. The derivation of spectral equations and the extraction of quantitative results[8] were facilitated by observing that the region of resonant tearing mode interaction is located well within the reversal surface, where $B_{oz} > B_{o\vartheta}$. Hence, conventional[9] reduced resistive MHD is an adequate plasma model. Using standard methods[10], it follows that the equations for kinetic and magnetic energies $E^K_{\underline{k}}$ and $E^M_{\underline{k}}$, where $\underline{k}=(m,n)$, are:

$$\frac{\partial E^k_{\underline{k}}}{\partial t} = i\int dx \varphi_{-\underline{k}}\, k_{\|} J_{\underline{k}} - \int dx\, \langle \varphi \nabla_{\vartheta} \psi \rangle_{\underline{k}} \langle J \rangle'$$

$$+ \int dx \sum_{\underline{k}'} \left(1 - \frac{n'^2}{n''^2}\right) \Delta'_{\underline{k}''} \frac{\delta(x'')}{\Delta\omega_{\underline{k}''}}\, I(\underline{k}', \underline{k}) \tag{4}$$

$$\frac{\partial E^M_{\underline{k}}}{\partial t} = i\int dx J_{-\underline{k}} k_{\|} \varphi_{\underline{k}} - \int dx \langle \hat{J}^2 \rangle_{\underline{k}} / S$$

$$+ \int dx \left\{ \sum_{\underline{k}'} \frac{n^2}{n''^2} \Delta'_{\underline{k}''} \frac{\delta(x'')}{\Delta\omega_{\underline{k}''}}\, I(\underline{k}, \underline{k}') \right.$$

$$\left. - \frac{\Delta'_{\underline{k}}}{\Delta\omega_{\underline{k}}} \delta(x) \sum_{\substack{\underline{p},\underline{q} \\ \underline{p}+\underline{q}=\underline{k}}} I(\underline{p}, \underline{q}) \right\} \tag{5}$$

where:

$$I(\underline{r},\underline{s}) = [<(\nabla_\vartheta\psi)^2>_{\underline{r}}<(\nabla_r\varphi)^2>_{\underline{s}}+<(\nabla_\vartheta\varphi)^2>_{\underline{r}}<(\nabla_r\psi)^2>_{\underline{s}}]$$

and $\Delta\omega$ is the nonlinear decorrelation frequency. Equations (4) and (5) indicate that m=1 mode saturation occurs when

$$-\int dx \sum_n <\varphi\nabla_\vartheta\psi>_{1,n}<J>'$$
$$= \int dx \sum_{n,n'} |\Delta'_{2,n''}| \frac{\delta(x'')}{\Delta\omega_{2,n''}} <(\nabla_\vartheta\psi)^2>_{1,n'}<(\nabla_r\varphi)^2>_{1,n}$$

i.e. when coupling (by interaction with neighboring m=1's) to stable m=2 modes ($\Delta'_{2,n''}=-|\Delta'_{2,n''}|<0$) balances growth due to $<J>'$ relaxation. The nonlinear decorrelation frequency $\Delta\omega$ is determined by the m=1 fluctuation level (since m=1 modes are the dominant fluctuations), and is $\Delta\omega\sim(\delta B/B_o)_{rms}/|\Delta'_2 a|^{1/2}$. Here n and n′ are the mode numbers for test (n) and background (n′) m=1's and $(\delta B/B_o)_{rms}$ is the root mean square m=1 fluctuation level in the RFP core. Energy coupled to m=2 is then scattered to $m\geq3$ by similar processes, and ultimately dissipated by resistive diffusion at small scales (large m,n). Analytical results indicate that a power law energy spectrum ($E_m\sim m^{-\alpha},\alpha\sim1$) characterizes the nonlinearly generated modes.

A physical interpretation of the saturation mechanism is that the multiple helicity interaction of neighboring m=1's with stable ($\Delta'<0$), driven m=2's generates a nonlinear $\underline{J}\times\underline{B}$ force which stabilizes the m=1 mode by opposing the growth of m=1 vorticity. Note that this scenario is the opposite of that discussed in Reference [11] where the nonlinearly driven mode has positive Δ', and the resulting nonlinear destabilization triggers the onset of the major disruption in tokamaks.

In order to obtain a quantitative estimate of the saturated m=1 fluctuation level, it is necessary to calculate the left side of Eq. (6). Since m=1 tearing modes do not exhibit a Rutherford phase and because the islands overlap for very modest fluctuation levels ($\delta B/B \sim 10^{-3}$ for $\varepsilon \lesssim 1/4$), a straightforward recourse is to calculate the driving term using linear eigenfunctions. One finds that $(\delta B/B_o)_{rms} \approx (\gamma_{m=1}\tau_A)/|\Delta_2' a|^{1/2}$, where $\gamma_{m=1}\tau_A \sim S^{-1/3}$ is the m=1 mode linear growth rate. However, a (more appropriate) nonlinear calculation of $\langle\varphi(\nabla_\vartheta\psi)\rangle_{1,n}$[13] and the inclusion of the effects of quasilinear flattening of $\langle J\rangle'$ may yield modifications to this result.

Numerical solution of the nonlinear, full incompressible MHD equations can be used to test and clarify aspects of the theory. The reliability of this type of calculation is extensively discussed in Reference [14]. Previous numerical calculations[15] indicated that multiple helicity coupling effects play a significant role in the nonlinear evolution and saturation of m=1 tearing modes in RFP. As an additional test here, in Figure 2, the temporal evolution of the m=1, n=12 mode kinetic energy including coupling to m=2, n=23 (through interaction with m=1, n=11) is compared to the m=1, n=12 kinetic energy evolution when the m=2, n=23 is omitted. It is apparent that multiple helicity coupling to m=2 plays a significant role in the nonlinear saturation of m=1 tearing modes in the RFP. Indeed, since the number of large m,n modes (the ultimate energy sink) retained in the numerical calculation is severely limited, the effects of multiple helicity interaction are probably considerably more significant than indicated by Figure 2. It is useful to note that the apparent discrepancy between these results and those reported by other investigators[16,17] is probably due to the unphysical aspect ratio ($\varepsilon\sim1$) used in their cylindrical geometry calculations. Noting that $(\delta B_r/B_o)\cong\varepsilon/n^2rq'\sim\varepsilon^2$ is required for island overlap, it is clear that taking $\varepsilon\sim1$ implies that an unphysically large fluctuation level is necessary (for overlap). This misrepresents the actual dynamics by diminishing the effects of multiple helicity interaction. An extensive discussion of the numerical calculations, including comparisons with studies of the tokamak disruption, is contained in Reference [14].

The results of the numerical calculations can also be used to reconcile the theoretical prediction of the nonlinear generation of fluctuations with $m\geq2$,[8] with the experimental observation that nearly all the fluctuation power spectrum has m=0 or m=1 (including harmonics generated by toroidal distortion).[1] In Figure 3, $\tilde{B}_\vartheta(r)/B_o$ (obtained from the numerical solution) for m=1, n=11,12, and m=2, n=23 are plotted as a function of radius. Note that the m=2 $\tilde{B}_\vartheta$ fluctuation is much more localized than the m=1 fluctuation, and that, near the wall, $(\tilde{B}_\vartheta)_{m=2}/(\tilde{B}_\vartheta)_{m=1} < 10^{-2}$. Thus, it is not surprising that magnetic coil arrays located outside the liner, or (in the case of internal probes) at the edge of the plasma, detect comparatively little $m \geq 2$ signal.

3.2 Quasilinear Dynamics of Magnetic Fields

Experimental evidence has linked dynamo events (increases in $|\langle B_z \rangle|$ near r_{wall}) to m=1 MHD activity.[4] Due to their large radial extent and comparatively high fluctuation levels, it is not surprising that m=1 tearing modes can induce significant magnetic field profile modification. Their effects on the evolution of the average toroidal field $\langle B_z(r) \rangle$ at and beyond the reversal surface, and on the safety factor q_o (on axis) are of particular interest.

An understanding of profile modification effects requires a quantitative estimate of $\langle \hat{\underline{V}} \times \hat{\underline{B}} \rangle$, the average electric field induced by turbulence (m=1 modes).[8,17] Since the phenomena of interest occur at radii away from the m=1 resonance surfaces in the core, a (renormalized) quasilinear calculation of $\langle \hat{\underline{V}} \times \hat{\underline{B}} \rangle$, using the exterior region, ideal MHD equation $\hat{\underline{B}} = \underline{\nabla} \times \hat{\underline{\xi}} \times \langle \underline{B} \rangle$ to relate $\hat{B}$ to displacement $\hat{\xi}$, is valid. When $\hat{\xi}$ has the form of a kink displacement, the average poloidal electric field $\langle E_\vartheta \rangle$ induced by (m=1) turbulence and resistive diffusion near the reversal surface r_o is given by:

$$\langle E_\vartheta(r) \rangle = -\Big(\sum_n \Big[(1-nq(r)) \frac{|\hat{\xi}_{1,n}(r)|^2}{r} \Delta\omega_{1,n} \Big] \langle B_\vartheta(r) \rangle$$

$$- \frac{1}{S} \langle J_\vartheta(r)\rangle\} \tag{7a}$$

and near r_{wall} is given by

$$\langle E_\vartheta(r)\rangle = - \{(\sum_n [\frac{\partial}{\partial r} |\hat{\xi}_{1,n}(r)|^2]\Delta\omega_{1,n})\langle B_z(r)\rangle$$

$$- \frac{1}{S} \langle J_\vartheta(r)\rangle\} \tag{7b}$$

where $\hat{\xi}(r)$ is the radial displacement and $\underline{\hat{v}}=\Delta\omega\underline{\hat{\xi}}$. It is important to recall that $\Delta\omega$ refers to the decorrelation rate for the saturated, stationary turbulence, and <u>not</u> the linear growth rates of the m=1 modes. Faraday's law $(\partial\langle\underline{B}(r)\rangle/\partial t=-\underline{\nabla}\times\langle\underline{E}(r)\rangle)$ shows that the condition for the <u>local</u> balance of turbulent generation of $\langle B_z(r)\rangle$ with decay by resistive diffusion is simply $\langle E_\vartheta(r)\rangle=0$.

Equations (7a,b) indicate that when (i) $\partial\langle B_z(r)\rangle/\partial r < 0$ and $q(r)<1/n$ $(dq/dr<0$ in RFP) at the reversal surface, and (ii) $\partial|\hat{\xi}_{1,n}(r)|^2/\partial r<0$ and $\langle B_z(r)\rangle$ is reversed at the wall, then; $\langle E_\vartheta(r)\rangle\to 0$ for $(\hat{\xi})_{rms}\sim(S\Delta\omega)^{-1/2}$. Thus, m=1 tearing mode fluctuation levels of $(\hat{\xi})_{rms}\sim(\delta B/B_o)_{rms}\sim S^{-1/3}$ and $\Delta\omega\sim S^{-1/3}$ (which are consistent with the results of Section 3.1) can induce modifications in $\langle B_z(r)\rangle$ which offset resistive diffusion, thus maintaining the magnetic configuration.

Some physical insight into the dynamo mechanism may be obtained by examination of the $\hat{z}$ component of the curl of Eq. (7a), which implies that $\partial\langle B_z\rangle/\partial t-(1/S)\nabla_r^2\langle B_z\rangle\approx\alpha\langle J_z\rangle$, where $\alpha = \sum_n (1-nq(r))|\hat{\xi}_{1,n}(r)|^2\Delta\omega_{1,n}/r$. Thus, it is apparent that helical m=1 modes "twist" toroidal current into the poloidal direction, thus generating $\langle B_z(r)\rangle$ acording to an α-effect[18] relation. The directional asymmetry necessary for this α-effect is a consequence of the radial dependence of $k_\parallel$ ($dq/dr<0$) imposed by the magnetic configuration structure. Also, in the RFP, global m=1 modes convert poloidal field magnetic energy density (tapped at the mode resonance surfaces in the core) into toroidal field energy density. Thus, the RFP dynamo is merely a process of <u>redistribution</u> of magnetic energy and current density, and must be maintained by an external driving agent, such as the toroidal electric field.

A very important feature of the quasilinear dynamics of m=1 tearing modes in RFP is that they cause a decrease in the value of q(0). Near the origin, the evolution of q is given by[17]

$$\frac{\partial q}{\partial t} \approx \frac{dq}{dr} \sum_n \frac{\Delta\omega_{1,n}}{r} \, |\hat{\xi}_{1,n}(r)|^2 \tag{8}$$

Thus, the m=1 modes tend to stabilize themselves by lowering q(0), thereby pushing their resonant surfaces into the origin. This process is another possible m=1 mode saturation mechanism. Hence, while resistive diffusion away from a Taylor state destabilizes the m=1 modes, the finite amplitude fluctuations act to oppose this trend and stabilize themselves by <u>lowering</u> q(0) and, in the process, drive $\langle B_z\rangle$ toward reversal. Since the competing effects balance for $(\hat{\xi})_{rms} \sim (S\Delta\omega)^{-1/2} \sim S^{-1/3}$ for $\Delta\omega \sim S^{-1/3}$, it is not surprising that full nonlinear and quasilinear numerical calculations reveal qualitatively similar temporal evolution of F and ϑ, while exhibiting grossly different fluctuation dynamics. Finally, it should be emphasized that quasilinear theory alone does <u>not</u> sufficiently characterize the saturated state.

4. NONLINEAR INTERACTION OF RESISTIVE INTERCHANGE MODES

The RFP is characterized by strong shear, average unfavorable curvature, and high β_p, where typically $\beta_p \sim 10\%$. Hence, it is not surprising that the resistive interchange mode has been proposed as a candidate for the explanation of the observed magnetic fluctuations and confinement deterioration in RFP. Previous[19] and contemporary[20] investigations have been primarily computational[19], or are based on simple dimensional analysis.[20] Here, the results of an analytical investigation[21] of resistive pressure driven turbulence are summarized and compared to the results of particle simulation. The basic approach is similar to that used in the study of resistive ballooning mode turbulence.[22]

The nonlinear dynamics of resistive interchange modes are most easily investigated using a simple electrostatic pressure convection model based on reduced MHD. Using Ohm's law to eliminate the current $J_\parallel$, it follows that the basic equations are:

$$\frac{\partial p}{\partial t} + \underline{\nabla}\varphi \times \underline{z} \cdot \underline{\nabla} p = -\nabla_\vartheta \varphi \, \partial \langle p \rangle / \partial r \tag{9}$$

$$\frac{\partial}{\partial t}\nabla_{\perp}^{2}\varphi + \underline{\nabla}\varphi\times\underline{z}\cdot\underline{\nabla}\nabla_{\perp}^{2}\varphi = -S\nabla_{\|}^{(0)2}\varphi - \kappa\nabla_{\vartheta}p \tag{10}$$

where p is the pressure, $\nabla_{\|}^{(0)} = \langle\underline{b}\rangle\cdot\nabla$, and κ is the curvature parameter ($\kappa>0$). The linear growth rate γ and radial mode width λ are $\gamma=S^{-1/3}(\kappa\langle p\rangle' k_{\|}')^{2/3}$ and $\lambda = S^{-1/3}(\kappa\langle p\rangle')^{1/6}(k_{\|}')^{-1/3}$, where $k_{\|}=k_{\|}'x$.

It is commonly believed that resistive interchange modes saturate when the turbulence level is sufficient to diffuse a parcel of pressure a distance λ in one growth time γ^{-1}, i.e. when $D=\gamma\lambda^{2}$, where D is the diffusion coefficient for turbulent convection. To examine this mixing length theory, renormalized fluid equations for $p_{\underline{k}}$ and $\nabla_{\perp}^{2}\varphi_{\underline{k}}$,

$$\frac{\partial p_{\underline{k}}}{\partial t} - \frac{\partial}{\partial x} D \frac{\partial}{\partial x} p_{\underline{k}} = -ik_{\vartheta}\langle p\rangle'\varphi_{\underline{k}} \tag{11}$$

$$\frac{\partial}{\partial t}(\nabla_{\perp}^{2}\varphi)_{\underline{k}} - \frac{\partial}{\partial x} D \frac{\partial}{\partial x}(\nabla_{\perp}^{2}\varphi_{\underline{k}}) + k_{\vartheta}^{2}C_{\underline{k}}\varphi_{\underline{k}}$$

$$= Sk_{\|}'^{2}x^{2}\varphi_{\underline{k}} - i\kappa k_{\vartheta}p_{\underline{k}} \tag{12}$$

have been derived. Here $D = \sum_{\underline{k}'} k_{\vartheta}'^{2}\langle\varphi^{2}\rangle_{\underline{k}'}/\Delta\omega_{\underline{k}''}$ is the fluid turbulence diffusion coefficient, and $C_{\underline{k}}= \sum_{\underline{k}'} \langle(\nabla_{\perp}^{2}\hat{\varphi})^{2}\rangle_{\underline{k}'}/\Delta\omega_{\underline{k}''}$, a term which is a consequence of symmetrization, ensures that the energy conserving property $\int d^{3}x\varphi(\nabla\varphi\times\underline{z}\cdot\nabla\nabla_{\perp}^{2}\varphi)=0$ is preserved in the renormalized theory. Thus, the kinetic energy evolves according to:

$$\frac{\partial E^k}{\partial t} = -\int dx \sum_{\underline{k}} \{k_\parallel'^2 x^2 S|\varphi_{\underline{k}}|^2 - i\kappa k_\vartheta \varphi_{-\underline{k}} p_{\underline{k}}\} \tag{13}$$

where $\partial E^k/\partial t=0$ at saturation. Note that the resistive field line bending term $\sim k_\parallel'^2 x^2 S$ damps the growth of E^k, and opposes the drive due to $\langle p\rangle'$ relaxation. The saturated state may be characterized by the diffusion coefficient D and a nonlinear mixing length $\Delta_{\underline{k}}$. The asymptotic balance of the anomalous viscosity (voriticity diffusion) and (resistive) field line bending terms of Eq. (12) implies that $\Delta_{\underline{k}}=(k_\parallel'^2 S/D)^{-1/6}$. Taking $p_{\underline{k}}\simeq -ik_\vartheta\langle p\rangle'\varphi_{\underline{k}}/(D/\Delta_{\underline{k}}^2)$, $k_\parallel'^2 x^2 S \simeq k_\parallel'^2\ \Delta^2_{\underline{k}} S$ and requiring $\partial E^k/\partial t=0$ yields $D=\kappa\langle p\rangle' L_s^2/S$ and thus, by substitution, $\Delta_{\underline{k}}=S^{-1/3}(\kappa\langle p\rangle')^{1/6}(k_\parallel')^{-1/3}$. Note that $\Delta_{\underline{k}}=\lambda$ and $D=\gamma\lambda^2$. Thus, the simple mixing length theory is vindicated. Noting that $\Delta\omega_{\underline{k}}\sim D/\Delta_{\underline{k}}^2$, it follows that the electrostatic fluctuation level is $(e\varphi/T_e)_{rms}\sim(D/\rho_s c_s k_\vartheta \Delta_{\underline{k}})_{rms}$ and, using Ohm's law, $(\delta B_r/B_o)_{rms}\sim\beta_p^{4/3}S^{-2/3}$.

A three dimensional electrostatic particle simulation[23] has been used to investigate the nonlinear, multiple helicity interaction of resistive interchange modes in a sheared slab, where curvature is modeled by a gravity force. In Figure 4, the n–averaged value of $e\varphi_m/T_e$ obtained from the simulation results is plotted versus m. Agreement with the prediction of mixing length theory is good. Extensions to the regime of large diamagnetic frequency ($\omega_{*e}>\gamma$) are in progress.

5. ANOMALOUS THERMAL TRANSPORT AND SCALING LAWS

Experimental evidence has linked heat transport along stochastic magnetic field line generated by the overlap of m=1 tearing modes with confinement in the HBTXIA pinch.[1] Using the saturated state magnetic fluctuation level obtained in Section 3, a quasilinear estimate of the (collisionless) thermal conductivity χ_E in the core region is $\chi_E \sim (.01) v_{Te} a S^{-2/3}$, where v_{Te} is the electron thermal velocity. Balancing heat loss with ohmic heating yields (for plasma density proportional to current I_p) $T_e \sim I_p^{.7}$. For $S \sim 10^5$, $\beta_p \sim 10\%$ is predicted. The temperature scaling and β_p value are in reasonable agreement with experiment.

In comparison, following the procedure of Reference [22], the (collisionless) electron thermal conductivity which results from magnetic fluctuations driven by resistive interchange modes is $\chi_E \sim (\varepsilon/q)^3 \beta_p^{3/2} v_{Te} a/S$. Balancing heat loss with ohmic heating yields (for density proportional to I_p) $T_e \sim I_p$ and $\beta_p \sim (q/\varepsilon)(m_e/m_i)^{1/6} \sim 10\%$. Thus, the thermal loss prediction for resistive interchange modes is qualitatively similar to that for m=1 tearing modes, but smaller in magnitude. Also, electromagnetic resistive interchange modes[19] and, especially near the plasma edge, rippling modes[24,25] may cause significant losses.

Acknowledgements

The authors are grateful to Drs. I. Hutchinson, C. Gimblett, A. Aydemir, E. Caramana, R. Gerwin, A. Hasegawa, C.S. Liu, R. Nebel, and D. Schnack for many useful conversations. This research was supported by the United States Department of Energy, Office of Fusion Energy under contracts DE–FG05–80ET–53088 with The Institute for Fusion Studies, DEAC05–84OR2 1400 with Martin Marietta Energy Systems, Inc., and DE–AC02–76ER03077 with New York University.

REFERENCES

[1] HUTCHINSON, I.H., et al., Nucl. Fusion 24 (1984) 59.

[2] WURDEN, G.A., Phys. Fluids 27 (1984) 554.

[3] LA HAYE, R.A., et al., Nucl. Fusion 21 (1982) 1235.

[4] WATT, R.G., NEBEL, R.A., Phys. Fluids 26 (1983) 1168.

[5] STRAUSS, H.R., "Dynamical Equations for the Reversed Field Pinch", (1983) submitted to Phys. Fluids.

[6] CARAMANA, E.J., et al., Phys. Fluids 26 (1983) 1305.

[7] TAYLOR, J.B., Phys. Rev. Lett. 33 (1974) 134.

[8] DIAMOND, P.H., et al., Institute for Fusion Studies Report #136 (1984).

[9] STRAUSS, H.R., Phys. Fluids 19 (1976) 134.

[10] DIAMOND, P.H., et al., Phys. Fluids 27 (1984) 1449.

[11] CARRERAS, B.A., et al., Phys. Rev. Lett. 46 (1981) 1131.

[12] RUTHERFORD, P.H., Phys. Fluids 16 (1973) 1903.

[13] DIAMOND, P.H., AN, Z.G., Proc. of Annual Controlled Fusion Theory Conference, Paper 2P13 (1984).

[14] HICKS, H.R., et al., ORNL TM–9127 (1984).

[15] HOLMES, J.A., et al., I.F.S. Report #124 (1984).

[16] AYDEMIR, A., BARNES, D., Proc. of Annual Controlled Fusion Theory Conf., Paper 1D2 (1984).

[17] STRAUSS, H.R., "The Dynamo Effect in Fusion Plasmas" (1984).

[18] MOFFATT, H.K., "Magnetic Field Generation in Electrically Conducting Fluids" (1978) Cambridge University Press.

[19] HENDER, T.C., ROBINSON, D.C., Plasma Physics and Controlled Nuclear Fusion Research 1982, Vol. III, 417.

[20] CONNER, J.W., TAYLOR, J.B., Paper IAEA–CN–44/E–I–2, these proceedings.

[21] AN, Z.G., DIAMOND, P.H., Proc. of 6th U.S. Symposium on Compact Toroid Research, Princeton Plasma Physics Laboratory, (1984) to be published.

[22] CARRERAS, B.A., et al., Phys. Rev. Lett. 50 (1983) 503.

[23] SYDORA, R.D., et al., I.F.S. Report 125 (1984).

[24] CALLEN, J.D., et al., Plasma Physics and Controlled Nuclear Fusion Research 1982, Vol. 1, 297.

[25] GARCIA, L., et al., I.F.S. Report #146 (1984).

FIGURE CAPTIONS

1. a) RFP $q(r)$ profile with location of resonances (not to scale). b) Location of primary ($m=1$) and nonlinearly driven ($m=2$) modes (not to scale).

2. Comparison of kinetic energy evolution with and without $m=2$ coupling.

3. Comparison of radial structure of $m=1$ and nonlinearly driven $m=2$ modes.

4. Comparison of fluctuation level from simulation with mixing length theory for resistive interchange mode saturation level.

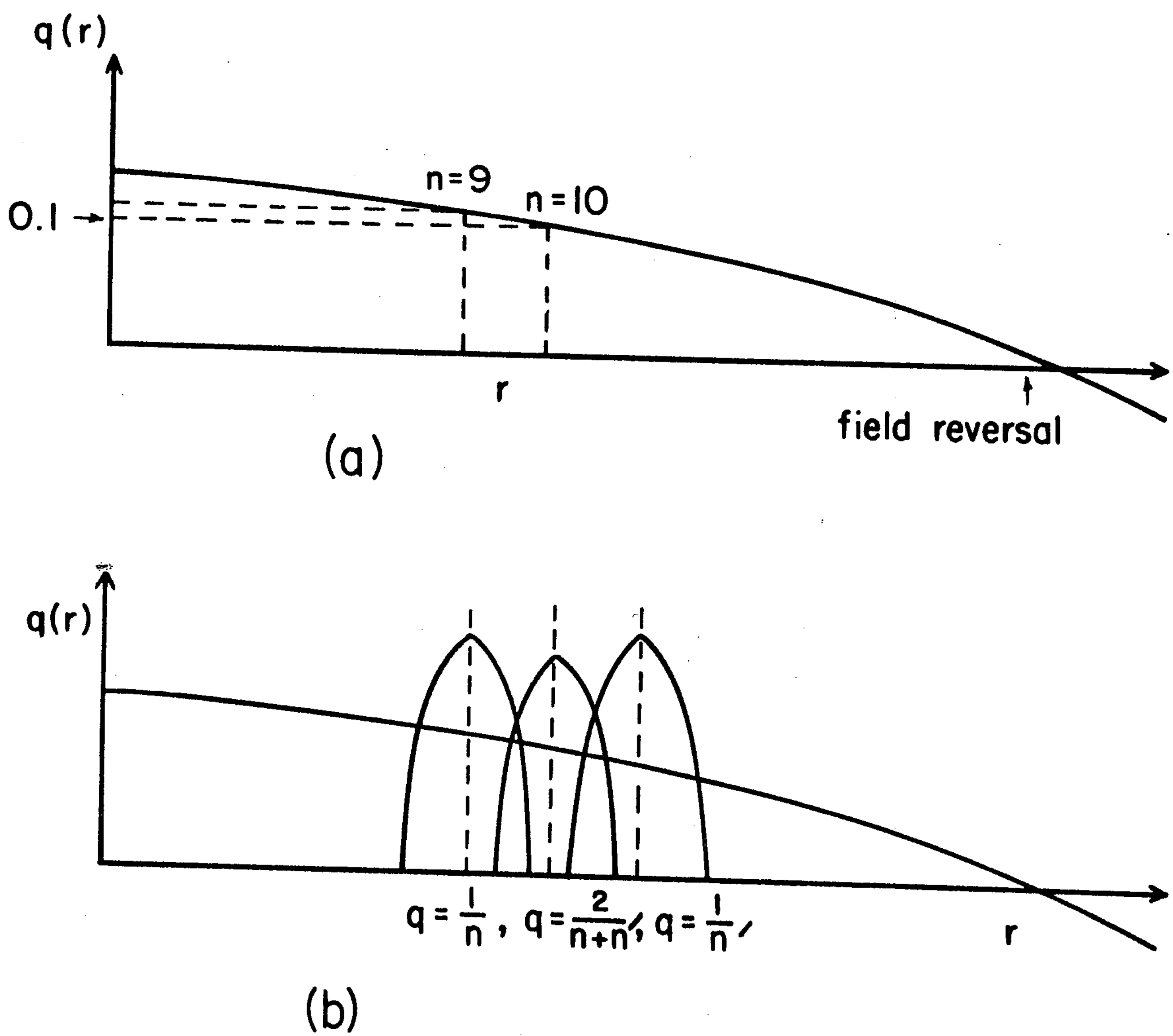

FIGURE 1

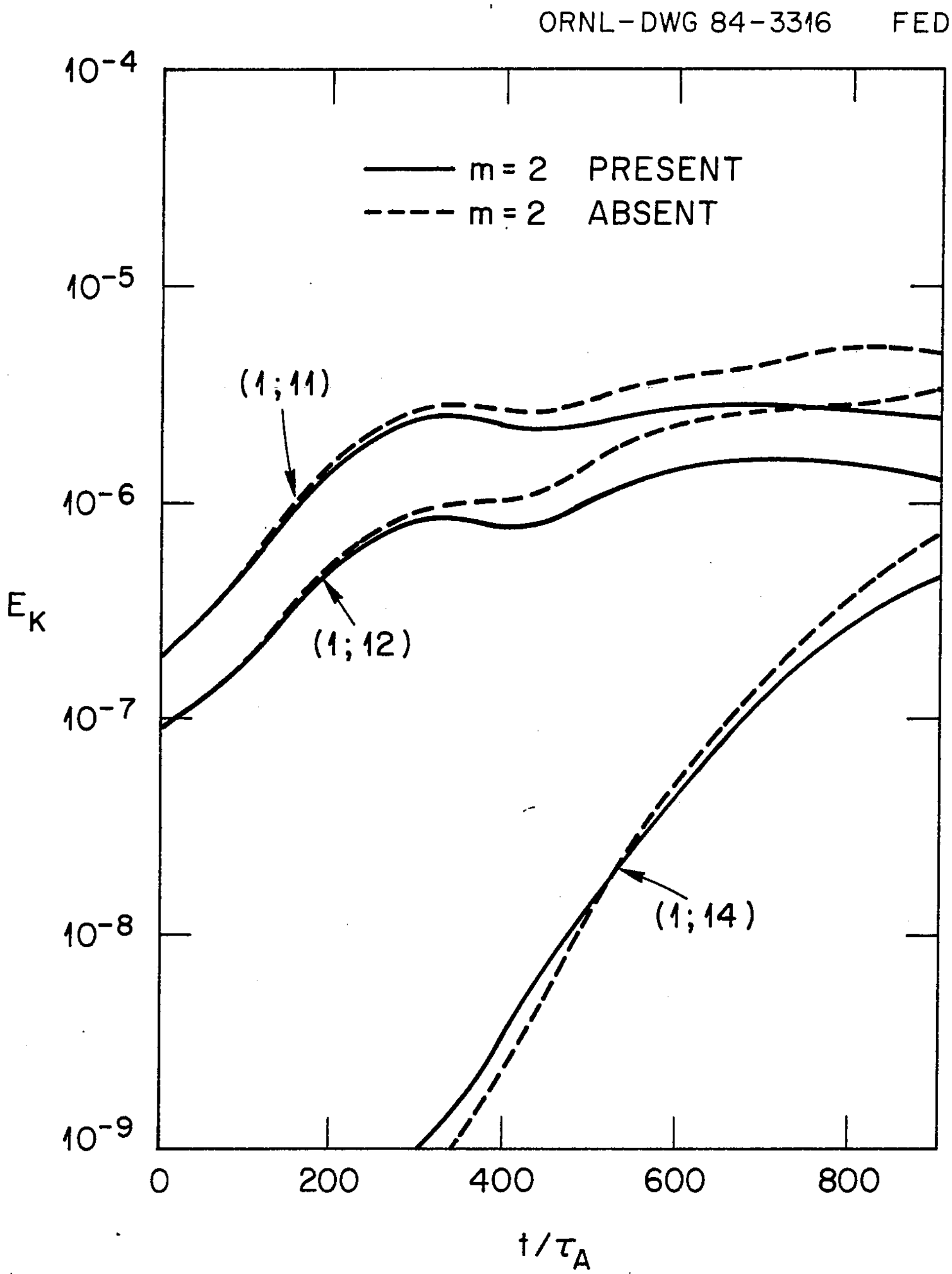
ORNL-DWG 84-3316 FED
10^{-4}
10^{-5}
10^{-6}
10^{-7}
10^{-8}
10^{-9}
m = 2 PRESENT
m = 2 ABSENT
(1; 11)
(1; 12)
(1; 14)
E_K
0
200
400
600
800
t/τ_A

FIGURE 2

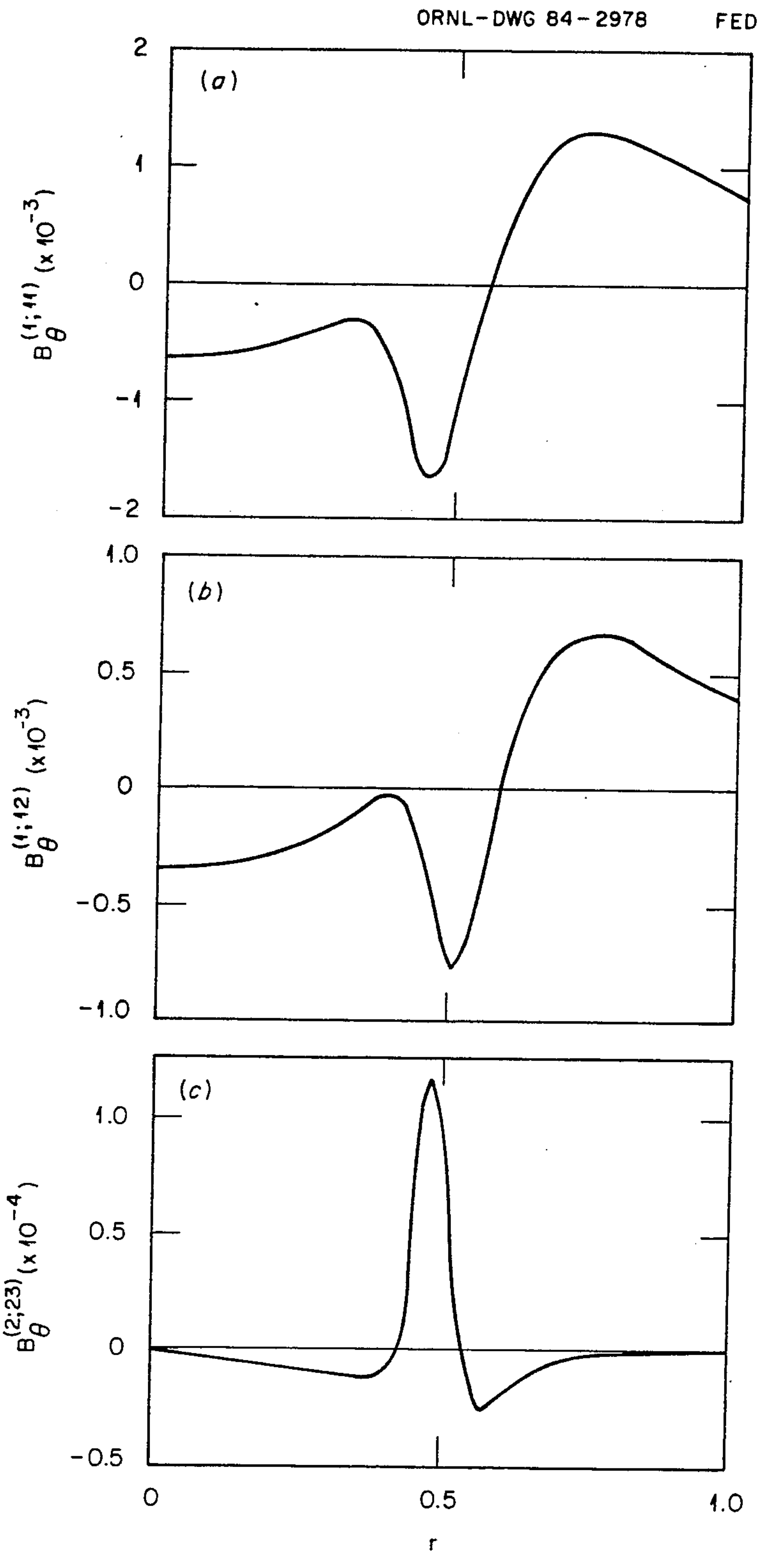
ORNL-DWG 84-2978 FED
(a)
$B_\theta^{(1;11)}$ (x10^{-3})
2
1
0
-1
-2
(b)
$B_\theta^{(1;12)}$ (x10^{-3})
1.0
0.5
0
-0.5
-1.0
(c)
$B_\theta^{(2;23)}$ (x10^{-4})
1.0
0.5
0
-0.5
0
0.5
1.0
r

FIGURE 3

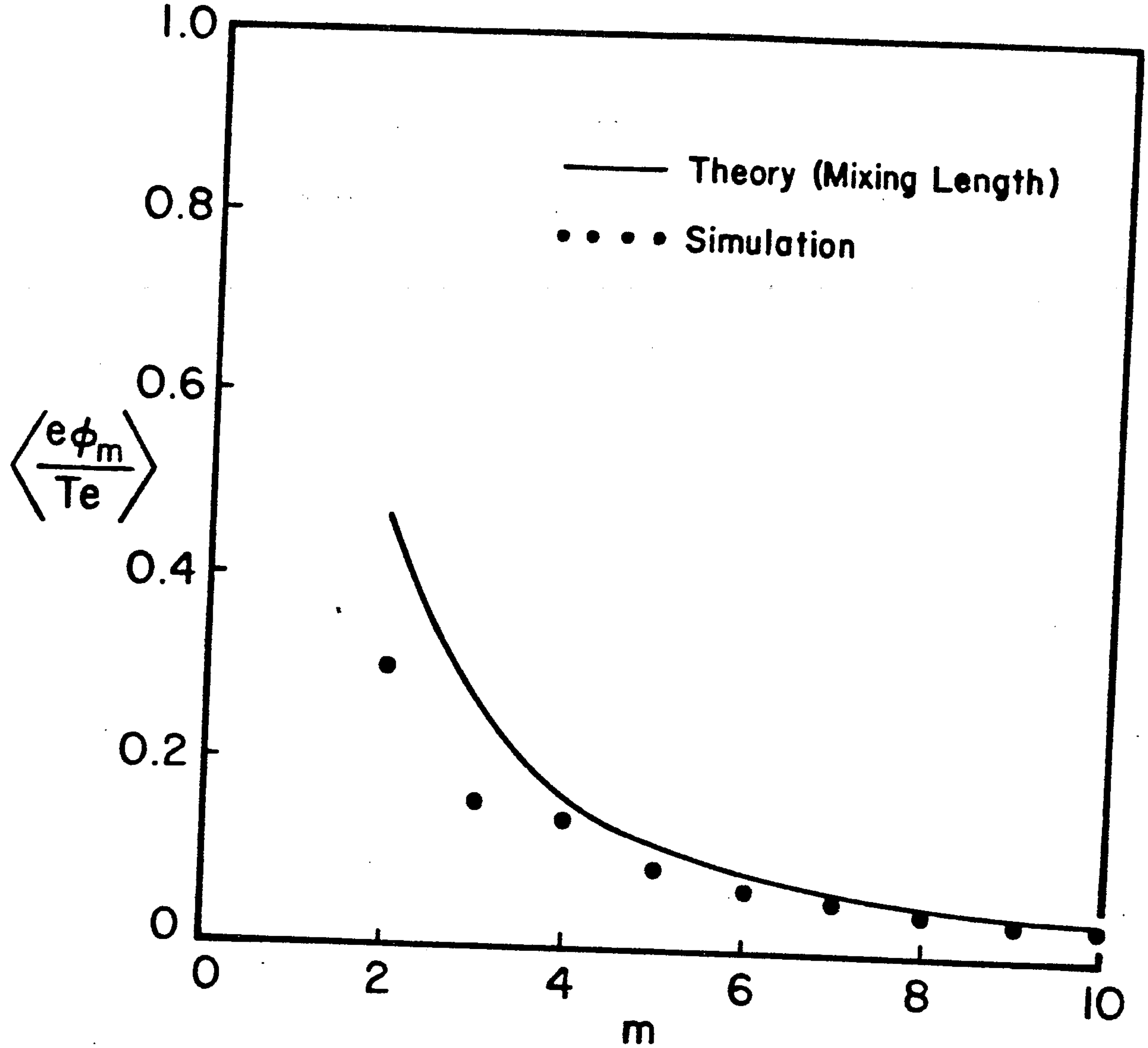
1.0
0.8
0.6
0.4
0.2
0
$\left\langle \frac{e\phi_m}{Te} \right\rangle$
Theory (Mixing Length)
Simulation
0
2
4
6
8
10
m

FIGURE 4